Available online at www.sciencedirect.com
ScienceDirect
Journal of Contaminant Hydrology 90 (2007) 41–57
JOURNAL OF Contaminant Hydrology
www.elsevier.com/locate/jconhyd

An interpretation of potential scale dependence of the effective matrix diffusion coefficient

H.H. Liu [a,*], Y.Q. Zhang [a], Q. Zhou [a], F.J. Molz [b]

[a] *Earth Sciences Division, Lawrence Berkeley National Laboratory, Berkeley, California, United States*
[b] *Department of Environmental Engineering and Science, Clemson University, Clemson, South Carolina, United States*

Received 23 November 2005; received in revised form 5 September 2006; accepted 11 September 2006
Available online 25 October 2006

Abstract

Matrix diffusion is an important process for solute transport in fractured rock, and the matrix diffusion coefficient is a key parameter for describing this process. Previous studies have indicated that the effective matrix diffusion coefficient values, obtained from a large number of field tracer tests, are enhanced in comparison with local values and may increase with test scale. In this study, we have performed numerical experiments to investigate potential mechanisms behind possible scale-dependent behavior. The focus of the experiments is on solute transport in flow paths having geometries consistent with percolation theories and characterized by multiple local flow loops formed mainly by small-scale fractures. The water velocity distribution through a flow path was determined using discrete fracture network flow simulations, and solute transport was calculated using a previously derived impulse-response function and a particle-tracking scheme. Values for effective (or up-scaled) transport parameters were obtained by matching breakthrough curves from numerical experiments with an analytical solution for solute transport along a single fracture. Results indicate that a combination of local flow loops and the associated matrix diffusion process, together with scaling properties in flow path geometry, seems to be an important mechanism causing the observed scale dependence of the effective matrix diffusion coefficient (at a range of scales).

Keywords: Matrix diffusion; Solute transport; Scale dependence; Fractured rock

1. Introduction

The exchange of solute mass (through molecular diffusion) between fluid in fractures and fluid in the rock matrix is called matrix diffusion. Direct laboratory and field evidence of matrix

* Corresponding author. Tel.: +1 510 486 6452.
E-mail address: hhliu@lbl.gov (H.H. Liu).

0169-7722/$ - see front matter © 2006 Elsevier B.V. All rights reserved.
doi:10.1016/j.jconhyd.2006.09.006

diffusion has been obtained in terms of an observed solute penetration distance into a rock matrix (e.g., Birgersson and Neretnieks, 1990; Jardine et al., 1999; Polak et al., 2003). Indirect evidence has been obtained from multi-tracer tests through the significant breakthrough-curve separation of simultaneously injected tracers of different matrix diffusion coefficient values (e.g., Maloszewski et al., 1999; Karasaki et al., 2000; Reimus et al., 2003a,b; Liu et al., 2004b). Owing to the orders-of-magnitude slower flow velocity in the matrix compared to that in fractures, matrix diffusion can significantly affect solute transport in fractured rock, and therefore is an important process for a variety of problems, including remediation of subsurface contamination and geological disposal of nuclear waste (e.g., Jardine et al., 1999; Neretnieks, 2002).

The matrix diffusion coefficient (molecular diffusion coefficient in free water, multiplied by matrix tortuosity) is an important parameter for describing matrix diffusion, and in many cases largely determines overall solute transport behavior. While matrix diffusion coefficient values measured from small rock samples in the laboratory are generally used for modeling field-scale solute transport in fractured rock (Boving and Grathwohl, 2001), several research groups recently have independently found that effective matrix diffusion coefficients much larger than laboratory measurements are needed to match field-scale tracer test data (Becker and Shapiro, 2000; Shapiro, 2001; Neretnieks, 2002; Liu et al., 2003, 2004a).

In the past, the observed enhancement of the effective matrix diffusion coefficient has been attributed to different mechanisms. Shapiro (2001) suggested that large-scale "effective matrix diffusion" is not a diffusive process, but actually an advective process between high and low permeability zones, resulting in a significantly increased "effective diffusion coefficient." Neretnieks (2002) argued that the existence of fracture in-filling creates relatively large areas for solute to diffuse into rock matrix, which, together with the process of diffusion into stagnant water, contributes to the need for increasing the effective diffusion coefficient to match the data. Wu et al. (2004) and Liu et al. (2002, 2003, 2004a) indicated that the existence of many small-scale fractures (which considerably increase the fracture–matrix interface area, but are not considered in numerical models) might be the major reason for the relatively large effective diffusion coefficients calculated from field data. Zhou et al. (2006) demonstrated that the existence of a degradation zone (with a relatively large matrix porosity and effective matrix diffusion coefficient) near the fracture–matrix interface also contributes to the observed enhancement of effective matrix diffusion coefficient. Tsang and Doughty (2003) reported that the observed enhancement of the effective matrix diffusion coefficient might result from the existence of so-called complex fractures (Mazurek et al., 2001). These complex fractures are characterized as a thin fracture zone having several interconnected subfractures.

In addition to the observed enhancement, Liu et al. (2004b) reported that on the basis of field test results, the effective matrix diffusion coefficient might be scale dependent. Zhou et al. (2005) further reported the scale dependence by performing a more comprehensive review of related field-testing results. The effective matrix diffusion coefficient, like permeability and dispersivity, seems to increase with test scale. This scale dependence has important implications for large-scale solute transport in fractured rock. Although a number of mechanisms have been proposed to explain the enhancement of the effective matrix diffusion coefficient (mentioned above), mechanisms behind the scale dependence are not fully investigated nor quantified at this stage.

Liu et al. (2004b) argue that transport paths in a fracture network may display fractal properties, and therefore the fracture–matrix interface area (partially controlling the matrix diffusion process) would be scale dependent. Consequently, observed effective matrix diffusion coefficient values are also scale dependent. The major objective of this work is to develop a more rigorous interpretation of the scale dependence based mainly on fracture geometry. Specifically,

we focus on mass transfer among subfractures and the surrounding rock matrix associated with a single major flow path. Understanding this mass transfer process may hold the key to understanding why the effective matrix diffusion coefficient is scale dependent.

2. Methods

Numerical experiments are performed in this study to investigate mechanisms behind the observed scale dependence of the effective matrix diffusion coefficient. This section presents methodologies used in the numerical experiments.

2.1. A conceptual model of a water flow path in a fracture network

Water flow and solute transport processes in fractured rock are complicated by the involved heterogeneity at different scales and the complex geometry of fracture networks. Although different conceptual models for flow and transport in fractured rock exist, many studies indicate that a flow pattern is mainly characterized by many flow channels (or separate individual flow paths) (e.g., Tsang and Neretnieks, 1998). Different channels or paths have different flow and transport properties, resulting in large-scale heterogeneities. Water flow in a single flow path (or channel) has been often simplified as a flow process within a single straight fracture (e.g., Neretnieks, 2002; Becker and Shapiro, 2000). In reality, however, flow structure is more complicated than that, owing to the complexity of fracture network geometry. Percolation models (that study network connectivity and characteristics of cluster structures) provide more realistic representation of flow path geometry (e.g., Staffer and Aharony, 1994; Renshaw, 1999). For example, shown in Fig. 1 is a two-dimensional statistically isotropic bond percolation network at the percolation threshold (Renshaw, 1999). A bond can be considered as a single fracture within a fracture network. At percolation threshold, a network forms a single connected path from the inlet (top) to the outlet (bottom), as shown by heavy links in Fig. 1. Obviously, the backbone (consisting of heavy links) corresponds to an individual major flow path in a fracture network.

The backbone has several useful features. First, not all the bonds on the backbones are singly connected. It is clear from Fig. 1 (or other figures for bond percolation) that the singly connected

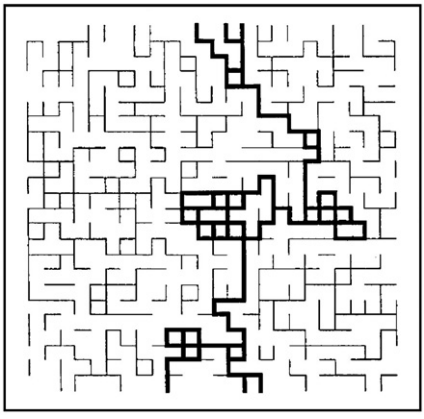

Fig. 1. A two-dimensional bond percolation network at the percolation threshold (after Renshaw (1999)). The heavy links correspond to the backbone.

segments are often separated by structures that contain several routes in parallel that are called *loops* by Staffer and Aharony (1994). As previously indicated, bonds in Fig. 1 can be considered as individual fractures (Renshaw, 1999). Therefore, these loops are also major features for flow pathways, as demonstrated, for example, by de Dreuzy et al. (2001) and Liu et al. (2002).

Second, it is well known that percolation structures at percolation threshold exhibit fractal scaling properties (Staffer and Aharony, 1994). This means that the cluster structure is similar (usually statistically similar) at different scales and the size of the loop will grow with the size of the network. However, when a percolation network is above percolation threshold, there exist multiple globally connected clusters (or flow paths) in a network. (The existence of multiple flow paths is more realistic for a natural fracture network.) In this case, the scaling properties are valid only for a scale smaller than the so-called correlation length defined as some average distance of the two bonds belonging to the same cluster (Staffer and Aharony, 1994). Roughly speaking, the correlation length is proportional to the size of a typical flow loop. The scaling will not exist anymore for a network with a size larger than the correlation length. In other words, the size of the loops cannot grow any further with scale when it approximately reaches the half spacing of the two separated flow paths.

Third, the above two features were originally observed for networks consisting of randomly distributed bonds with the same lengths. Networks of this kind are investigated in the classic percolation theories (Staffer and Aharony, 1994). However, real world fracture networks are generally more complicated, because of heterogeneity. Their distribution is not purely random and may exhibit spatial correlations and individual fractures are not identical. It is well documented that the trace length distribution of fractures follows a power law, and longer fractures generally have larger apertures (e.g., Renshaw, 1999; de Dreuzy et al., 2001; Liu et al., 2002). In this case, the two features mentioned above are still valid with additional complications (Renshaw, 1999; de Dreuzy et al., 2001; Liu et al., 2002; Darcel et al., 2003). As demonstrated in de Dreuzy et al. (2001) and Liu et al. (2002), singly connected parts of a flow path consist mainly of longer fractures with relatively large apertures, while the loops mainly result from intersections among large fractures and relatively short fractures. Note that aperture variability exists among these loops because fractures with different trace lengths are involved and fracture apertures, as mentioned above, are generally correlated to the fracture trace lengths.

It is also important to indicate that the above discussion is for bonds or fractures that form backbones for a network. There are some dead-end fractures or bonds connected to the backbone, as shown in Fig. 1. If there is a considerable advection process between fractures and the surrounding matrix, these dead-end fractures may be important for enhancing fracture–matrix interaction for solute transport (Wu et al., 2004). In this study, we ignore the effects of these dead-end fractures because the advection process between fractures and the surrounding matrix is extremely small, as a result of the negligible permeability value in the rock matrix under saturated flow conditions, i.e. the water within the dead-end fractures is essentially stationary. The more important features of a flow path corresponding to the backbone geometry of a fracture network (that are discussed above) are used in constructing our numerical experiments.

2.2. Numerical experiments

2.2.1. Construction of flow paths

Numerical experiments are designed to investigate solute transport processes through a flow path in a fracture network, with a focus on the effective matrix diffusion coefficient as a function of distance from the source. The flow paths are constructed to be consistent with the features discussed in Section 2.1. Fig. 2 shows a flow path constructed using a deterministic recursive procedure. The Level 1 fracture in Fig. 2 represents connected long fractures that form the singly

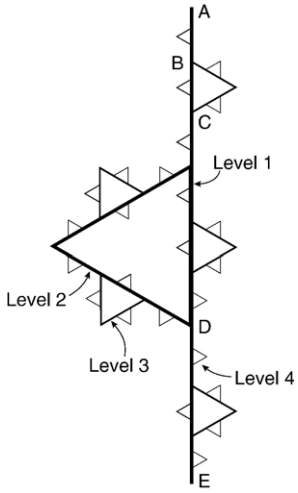

Fig. 2. A flow path characterized by scaling behavior.

connected segments in a network and the major conduit at locations where multiple loops exist. Two Level 2 fractures (with a shorter trace length and smaller fracture aperture than Level 1) are then added, and an equilateral triangle is formed where the loop occurs. The same procedure is continued to add Levels 3 and 4 fractures representing relatively small-scale fractures.

This recursive procedure enables a relatively small part of the flow path to be similar to the whole flow path in shape, an important feature of a fractal. As previously indicated, a flow path in a network at percolation threshold or within a scale less than the correlation length is fractal, but fractal scaling behavior no longer holds for a scale larger than the correlation length. To consider this nonfractal behavior at a relatively large scale, Fig. 3 presents a flow path constructed by removing the Level 2 fracture and those higher-level fractures connected to that fracture from

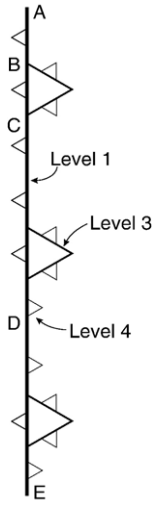

Fig. 3. A flow path generated by removing Level 2 fracture and the associated higher-level fractures from the path in Fig. 2.

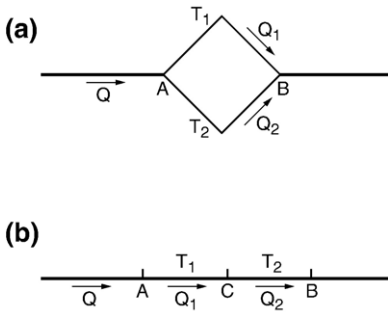

Fig. 4. Basic elements of a flow path that are used to calculate and distribute flow rates.

Fig. 2. By removing these fractures, the geometry of the flow path in Fig. 3 exhibits a scaling behavior at relatively small scales and a periodic (nonfractal) behavior at relatively large scales.

We set the length and the aperture of the Level 1 fracture in Figs. 2 and 3 to be 9 m and 0.001 m, respectively. Both of these values are consistent with the fracture data in the unsaturated zone of Yucca Mountain (BSC, 2004). Based on the consideration that longer fractures have larger fracture apertures, and that the hydraulic conductivity of a fracture is proportional to the square of the fracture aperture (e.g., de Marsily, 1986), hydraulic conductivity (K) and aperture (b) for different levels of fractures are assumed to have the following relation:

$$\frac{K_i}{K_{i+1}} = \left(\frac{b_i}{b_{i+1}}\right)^2 = \alpha \tag{1}$$

where $i=1$, 2 and 3 is the level of a fracture and $\alpha>1$ is a constant.

2.2.2. Calculation of water flow and solute transport

To calculate solute transport within a flow path, we need to calculate a steady-state flow rate (and velocity) for each segment in the path. Closed-form relations among a flow rate, the total water flow rate, and network properties can be obtained using relations derived from two basic elements (shown in Fig. 3) for a flow path. Defining the conductance to be the conductivity divided by the corresponding length of a given segment, we can express the total conductance (T_{ab}) from A to B and relations among flow rates in Fig. 4(a) as

$$T_{AB} = T_1 + T_2 \tag{2}$$

$$Q_1 = Q\frac{T_1}{T_{AB}} \tag{3}$$

$$Q_2 = Q\frac{T_2}{T_{AB}} \tag{4}$$

and for Fig. 4 (b) as

$$T_{AB} = \frac{1}{\frac{1}{T_1}+\frac{1}{T_2}} \tag{5}$$

$$Q_1 = Q_2 = Q \tag{6}$$

With these basic relations for flow in parallel and in serials, the flow rate in each segment can be derived. Note that water flow velocity is determined as the flow rate divided by the corresponding aperture. In this study, we set the total flow rate to be 0.001 m^2/day, corresponding to a water flow velocity on the order of 1 m/day for the Level 1 fracture (when flow rates at fractures of the other levels are ignored).

Once the flow field is determined, we calculate solute transport within a flow path to determine breakthrough curves at locations B, C, D, and E (Figs. 2 and 3). The calculations are based on recent theories to determine solute transport along a single flow pathway with a wide range of retention processes (including matrix diffusion) and spatially variable flow and transport properties (Cvetkovic et al., 2003; Painter and Cvetkovic, 2005). According to these theories, the impulse-response function in the time domain for such a single pathway system, which also may be viewed as the probability density distribution for a unit pulse input of conservative solute, is given as (Painter and Cvetkovic, 2005):

$$\gamma_l = \frac{H(t-\tau)B}{2\sqrt{\pi}(t-\tau)^{3/2}} \exp\left[\frac{-B^2}{4(t-\tau)}\right] \tag{7}$$

where H is the Heaviside function, and t is time. The residence time τ is defined by

$$\tau = \int_0^1 \frac{\mathrm{d}l}{V} \tag{8}$$

where l is the distance between the inlet and the location where a breakthrough curve is observed, and V is the water flow velocity along a flow pathway. The parameter B is defined as

$$B = \int_0^1 \frac{\phi\sqrt{D}}{b}\frac{\mathrm{d}l}{V} \tag{9}$$

where ϕ, D and b are the matrix porosity, local matrix diffusion coefficient (molecular diffusion coefficient multiplied by tortuosity factor), and local half aperture, respectively. The cumulative distribution of the impulse-response density (Eq. (7)), which will be used later, can be mathematically expressed as

$$C^*(t) = 0 \text{ for } t \leq \tau \tag{10-1}$$

$$C^*(t) = \mathrm{erfc}\left[\frac{1}{2}\frac{B}{(t-\tau)^{1/2}}\right] \text{ for } t > \tau \tag{10-2}$$

There are many different pathways between the inlet and the monitoring point for a given flow path (Figs. 1 and 2). Each pathway corresponds to a set of values for parameters τ and B. To determine these parameter values using Eqs. (8) and (9), we use a particle-tracking scheme. We release M particles from the inlet of a flow path, and track each particle from the inlet to the selected monitoring point. A particle moves with a local velocity at the given segment of the network; at an intersection the probability of a particle to move to a segment is determined as the ratio of flow rate for the segment to the total flow rate towards the intersection. In this study, we use M=5000. (Our numerical experiments showed that a larger M value gives essentially the same results as M=5000.) For solute transport with a constant concentration C_0 at the inlet, the

breakthrough curve at a monitoring point is given as an average over the particles of the superposition integral of the impulse–response function (Eqs. (10–1) and (10–2)), or

$$\frac{C(t)}{C_0} = \frac{1}{M}\sum_{i=1}^{M} C_i^*(t) \tag{11}$$

In this study, we set the matrix porosity ϕ at 0.1 and the local matrix diffusion coefficient D at 10^{-11} m^2/s, consistent with the corresponding data collected from the unsaturated zone of Yucca Mountain, Nevada (BSC, 2004; Wu et al., 2004). Also note that Eqs. (7), (8), (9), (10–1), (10–2) are valid only for cases in which fracture spacing is infinite, so that matrix diffusion is not limited by nearby fractures. Considering that the penetration depth of solute into the matrix is on the order of $\sqrt{Dt_{\text{test}}}$ (where t_{test} refers to the time when the last observation is made in a numerical experiment), and that this depth is generally much smaller than the smallest matrix block size in Figs. 1 and 2 (roughly characterized by the length of a segment for a level 3 fracture), these relations are here considered to be good approximations.

2.2.3. Determination of effective parameters

The effective parameters (including effective matrix diffusion coefficient) may be determined by fitting the numerical experiment results (Eq. (11)) to the analytical solution of Tang et al. (1981) for solute transport along a single fracture. A similar curve-fitting approach has often been used in interpreting field-scale tracer testing results. Also note that the analytical solution of Tang et al. (1981) was developed for the same boundary condition (constant concentration C_0 at the inlet) as that used to derive Eq. (11). The curve-fitting is conducted using iTOUGH2-TRAT (Zhou, 2005) by minimizing an objective function defined as the summation of the square of the differences (between a calculated concentration value and the corresponding concentration value observed from a numerical experiment) for different observation times. The iTOUGH2-TRAT program is based on iTOUGH2, a program using inverse modeling for parameter estimation (Finsterle, 1999).

Values for the three parameters, residence time τ, Peclet number $P_e = l/\alpha_L$ (where α_L is dispersivity) and parameter $A = \frac{\phi\sqrt{D_m}}{b}$ (where D_m is the effective matrix diffusion coefficient) are determined from fitting an observed breakthrough curve at a given monitoring location. The effective matrix diffusion coefficient is calculated from the fitted value of parameter A. To make sure that the global minima of the objective function to be obtained, corresponding to the best estimates of the related parameters, we used the computationally intensive grid research method during the curve-fitting process (Finsterle, 1999). The grid search refers to the systematic evaluation of the objective function in parameter space with parameter sets generated on a regular grid.

3. Results and discussion

Zhou et al. (2005) compiled the fitted effective matrix diffusion coefficients for different test sites reported in the literature and reanalyzed some tracer test results when the reported diffusion coefficient values are not available from the literature. Liu et al. (2004b) also conducted a less comprehensive literature survey. Based on these literature survey results, Liu et al. (2004b) and Zhou et al. (2005) indicated that the effective matrix diffusion coefficient for fractured rock, just like dispersivity and permeability, might be scale dependent and increase with test scale. Based on the fact that the effective matrix diffusion coefficient is proportional to the square root of the fitted

parameter A (Section 2.2.3), we define the following dimensionless parameter to characterize the possible scale-dependent behavior from numerical experiments:

$$D^* = \left(\frac{A}{A_{\text{ref}}}\right)^2 \tag{12}$$

where A_{ref} corresponds to the A value calculated using the local matrix diffusion coefficient and the aperture value for the Level 1 fracture. Obviously, D^* will change with travel distance from the source if the effective (fitted) matrix diffusion coefficient is scale dependent.

Under the methodology described previously, numerical experiments were performed for solute transport in the flow path shown in Fig. 2 for several α values including 5, 10, and 20. As indicated in Eq. (1), a larger α gives a smaller advective mass transfer from a low-level fracture to relatively high-level fractures. Fig. 5 shows matches of breakthrough curves numerically determined at locations B, C, D, and E in Fig. 2 for $\alpha = 10$, using the analytical solution for solute

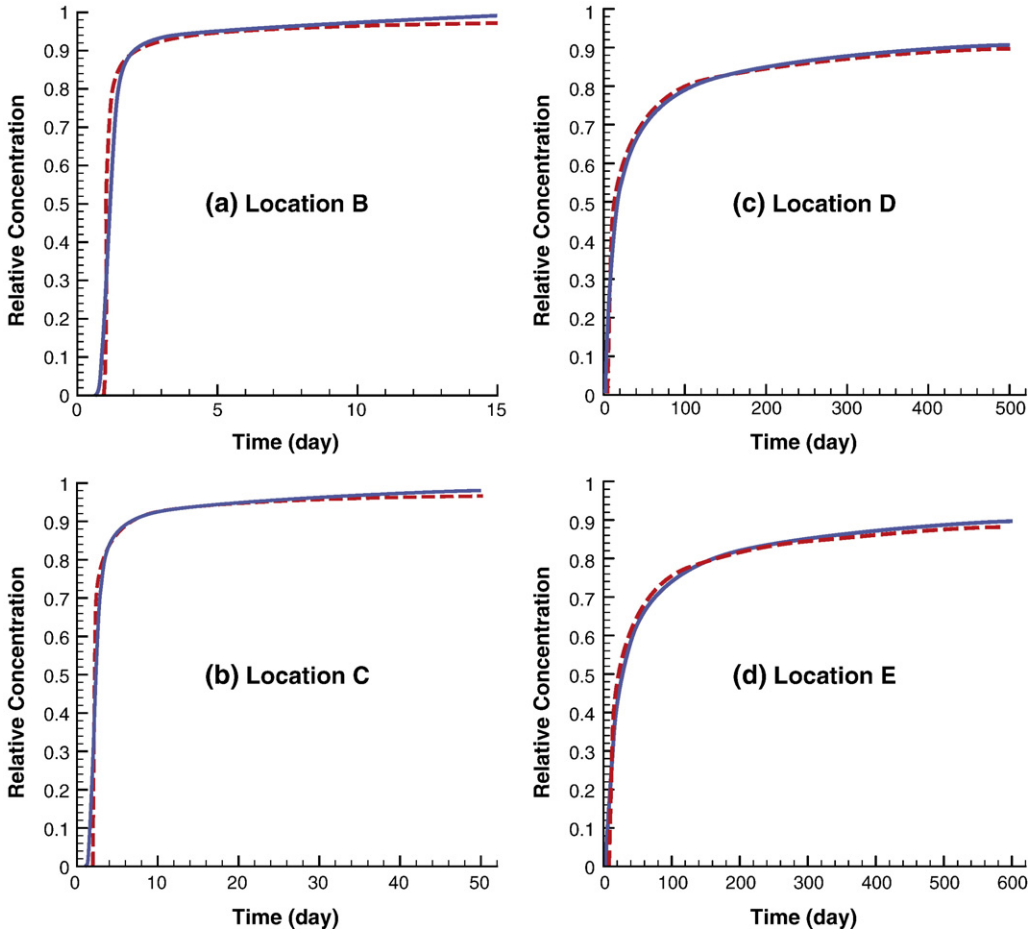

Fig. 5. Matches of numerical experiment results (dashed lines) with the analytical solution to solute transport through a single fracture (solid lines) at locations B, C, D and E for the flow path shown in Fig. 2.

transport in a single fracture. Similar matches are obtained for other α values. As previously discussed, this kind of match has been used in determining effective parameters, including the effective matrix diffusion coefficient. The distances from the source (location A) to locations B, C, D, and E are 1, 2, 6, and 9 m, respectively (Fig. 2).

Shown in Fig. 6 is the fitted effective matrix diffusion coefficient as a function of distance for the flow path in Fig. 2 and for $\alpha = 5$, 10, and 20, respectively. The effective matrix diffusion coefficient is indeed scale dependent and generally increases with distance. (The moderate decrease in the coefficient from D to E results from the fact that the largest flow loop in the flow path exists between C and D. If the size of the flow loop is much smaller than the size of flow path in the flow direction, the local decrease may disappear, as shown in Fig. 9.) For a given distance, the effective matrix diffusion coefficient generally decreases with increasing α, because a larger α reduces mass transfer from the Level 1 fracture to the other smaller fractures. For $\alpha = 100$ (not shown in Fig. 6), the D^* value is reduced to one and no scale dependence is detected. In this case, Level 2 and higher-level fractures essentially do not contribute to the flow and transport process. As expected, the determined residence time decreases with increasing α. For example, the residence times at Location E (Fig. 2) are 14, 12 and 10 days for $\alpha = 5$, 10, and 20, respectively. Fig. 7 also shows fitted dispersivity values for numerical experiments using the flow path in Fig. 2. The dispersivity increases with the travel distance, which is consistent with many studies reported in the literature (e.g., Neuman, 1990; Gelhar, 1993).

A combination of three mechanisms may contribute to the scale dependence of the effective matrix diffusion coefficient shown in Fig. 6. First, the scaling behavior of the flow path (i.e., the size of the flow loops and fracture matrix interface area increasing with scale) in Fig. 2 will generally give a larger degree of fracture matrix interaction at a larger scale. This results in a larger effective matrix diffusion coefficient at a larger scale. Note that the effective matrix diffusion coefficient may be related to the actual fracture–matrix interface area (Liu et al., 2004a). Second, the process of advective mass transport from Level 1 fractures to the other fractures forming flow loops in Fig. 2 is mathematically similar to matrix diffusion and may result in the scale dependence of the fitted effective matrix diffusion coefficient. (The similarity of this advective

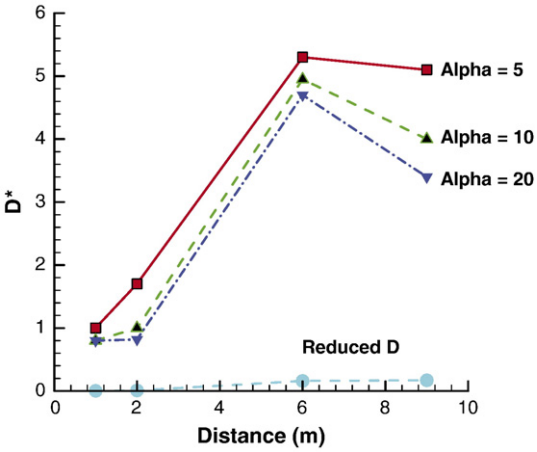

Fig. 6. Fitted relative effective matrix diffusion coefficient values (Eq. (12)) as a function of distance for the flow path shown in Fig. 2. The curve labeled with "reduced D" corresponds to the local matrix diffusion coefficient reduced by 100 times (as compared with the other curves).

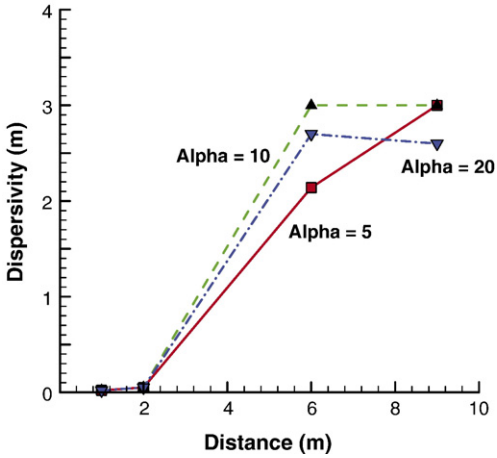

Fig. 7. Fitted dispersivity values as a function of distance for the flow path shown in Fig. 2.

transport process to matrix diffusion was used by Shapiro (2001) in interpreting certain field-scale testing data.) Third, matrix diffusion within these higher-level fractures may play an important role in determining the effective matrix diffusion coefficient (even when the scaling in geometry of a flow path does not exist). This diffusion process (which is not considered in the analytical solutions for estimating the effective matrix diffusion coefficient) may result in the observed scale dependence at a certain range of scales, because at a larger scale there are more solute particles traveling through small-scale fractures. Note that the effective matrix diffusion is inferred from parameter A (Section 2.2.3) and small fractures have large A values as a result of small apertures. This third mechanism is demonstrated in Fig. 8.

To check if the second mechanism (advective transport alone) is the dominant mechanism for the observed scale dependence, we conducted a numerical experiment using the flow path in Fig. 2 and for $\alpha = 5$. Specifically, we reduced the local matrix diffusion coefficient by 100 times. If the advective process were indeed the dominant mechanism, the effective matrix diffusion coefficient determined from the numerical experiments would not change significantly with the change in the local matrix diffusion coefficient. The determined effective matrix diffusion coefficients are also shown in Fig. 6. Obviously, values for these coefficients are significantly smaller than those with the higher local matrix diffusion coefficient (Fig. 6). Therefore, matrix diffusion within fractures including small-scale fractures, rather than the advective transport between fractures at different

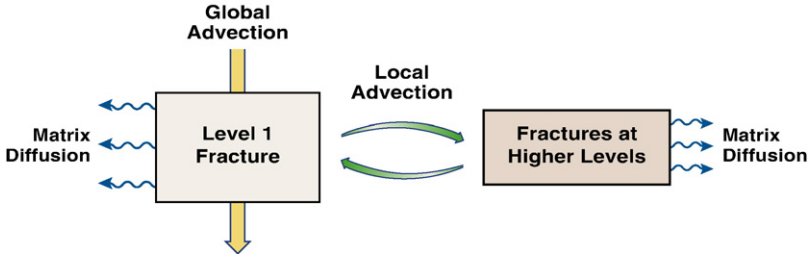

Fig. 8. Effective matrix diffusion as a combination of local-scale advection and matrix diffusion in fractures at different scales.

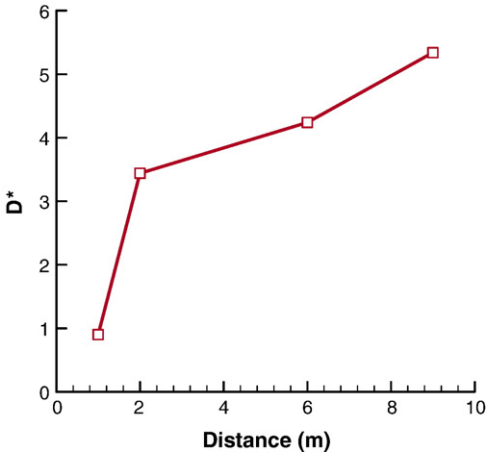

Fig. 9. Fitted relative effective matrix diffusion coefficient values (Eq. (12)) as a function of distance for the flow path shown in Fig. 3.

levels alone, is the ultimate process for determining the effective matrix diffusion coefficient and its scale dependence. However, advective transport to (high-level) small fractures is needed to move solute to these fractures from a Level 1 fracture for the matrix diffusion processes. Without this advection, matrix diffusion in these small fractures would not be able to occur.

As previously indicated in Section 2.1, the scaling of the network geometry for a flow path does not always exist especially when the size of a network is larger than the correlation length. To investigate the solute transport process in a network without scaling properties in geometry, we performed a numerical experiment using the flow path in Fig. 3 for $\alpha = 5$. The flow path does not have scaling properties in geometry at large scales. (As shown in Fig. 3, the scale under which the scaling in flow-path geometry holds is 3 m for this particular flow path.) Numerical experiment results observed at locations B, C, D and E (Fig. 3) are matched to determine values for the effective parameters (Section 2.2.3). As shown in Fig. 9, the effective matrix diffusion coefficient is still scale dependent for the given distance range from A to E. This seems to demonstrate that the existence of local flow loops and the associated matrix diffusion process can result in scale dependence for travel distances beyond the scale under which the scaling properties in geometry exist.

However, this study cannot exclude that a constant D^* can be reached for travel distances much larger than that from A to E (Fig. 3), owing to the lack of scaling properties in the flow path geometry at relatively large scales. The existence of the constant D^* at relatively large scales may be similar to the asymptotic behavior of macroscopic dispersivity for a flow field characterized by a stationary random permeability distribution (Frind et al., 1987; Gelhar, 1993). While the focus of this study is on possible mechanisms behind the observed scale dependence of the effective matrix diffusion coefficient, we will leave the potential asymptotic behavior of D^* at much larger scales to future research.

The above discussions indicate that a combination of local flow loops, matrix diffusion associated with these loops, and scaling properties in flow-path geometry, seems to be a major mechanism causing the scale dependence of the effective matrix diffusion coefficient observed at a range of scales. The scaling properties in flow-path geometry causes the increase in D^* at scales within which scaling holds. The matrix diffusion processes associated with flow loops result in

Table 1
Fitted parameter values for the first flow path (Fig. 2)

α	Location	D^*	τ (day)	α_L (m)
5	B	0.89	1.03	0.02
	C	1.73	2.00	0.05
	D	5.34	10.89	2.22
	E	5.10	14.00	3.00
10	B	0.76	1.03	0.02
	C	0.95	2.07	0.05
	D	4.91	9.00	3.00
	E	3.96	11.89	3.00
20	B	0.76	1.03	0.02
	C	0.82	2.08	0.05
	D	4.62	6.93	2.70
	E	3.34	10.00	2.57

further increases in D^* at relatively large scales. The advective process within flow loops is responsible for feeding solute into matrix diffusion processes within the related subfractures.

Tables 1, 2 and 3 give values for the fitted (effective) transport parameters for different numerical experiments. Because both dispersion and matrix diffusion processes can cause the spreading in the observed breakthrough curves, one may be concerned with the possibility that the scale dependence of the effective matrix diffusion coefficient is an artificial effect of the scale dependence of the dispersivity. This is not the case here. For example, Sánchez-Vila and Carrera (2004) theoretically demonstrated that the artificial matrix diffusion coefficient (when dispersion is completely ignored in the model) resulting from the actual dispersion process is inversely proportional to the dispersivity. Because the dispersivity increases with travel distance, one would not observe an increase in matrix diffusion coefficient with scale if the dispersion were artificially considered a major component of matrix diffusion process. The above argument is also supported by our simulation results showing a strong dependence of the effective matrix diffusion coefficient on the local diffusion coefficient.

The importance of flow-path geometry for the effective matrix diffusion coefficient values determined from the field tests based on simplified flow geometry is supported by the recent study by Neretnieks and Moreno (2003). They reported that matrix diffusion coefficient values much larger than the lab data were needed to match the results of tracer tests conducted at Äspö Hard Rock Laboratory in previous studies. Based on high-resolution transmissivity measurements in five boreholes at the test site, they concluded that there were many more conductive fractures than those assumed in previous studies. By including these new small-scale fractures with relatively small permeability values, they were able to reasonably reproduce the tracer test results with matrix diffusion coefficient values measured from the rock matrix samples. This is consistent with the concept that effective (large-scale) dispersivity for a natural porous medium can always be

Table 2
Fitted parameter values for the first flow path with the reduced local-scale diffusion coefficient value (Fig. 2)

α	Location	D^*	τ (day)	α_L (m)
20	B	0.0004	1.01	0.0008
	C	0.01	2.03	0.0016
	D	0.17	9.26	0.28
	E	0.18	12.00	0.21

Table 3
Fitted parameter values for the second flow path (Fig. 3)

α	Location	D^*	τ (day)	α_L (m)
5	B	0.90	1.03	0.02
	C	3.44	1.98	0.12
	D	4.24	4.68	0.24
	E	5.34	6.81	0.41

expressed in terms of a local value in a numerical model, provided that heterogeneity can be adequately resolved. However, it is practically difficult, if not impossible, to characterize fractures at different scales (or heterogeneity at different scales for porous media) for large-scale problems. Nevertheless, Neretnieks and Moreno (2003) demonstrated that small-scale fractures are indeed an important factor contributing to the differences between lab-scale and field-scale effective matrix diffusion coefficient values, which is consistent with our study results here.

Fig. 10 shows a comparison between our simulated results for the two flow paths and a portion of data points reported by Zhou et al. (2005) who surveyed effective matrix diffusion coefficient values from different test sites with test scales up to more than 1000 m. The parameter Fd refers to the ratio of the effective matrix diffusion coefficient value to its local-scale value, and is equivalent to D^* (Eq. (12)) for this specific study. The data points correspond to those from non-Granite fractured rock (with test scales less than 100 m) because our simulations are roughly based on parameter values from the unsaturated zone of Yucca Mountain that is not Granite. For a given travel distance (test scale) in the figure, the simulation result refers to the average D^* values for the two flow paths shown in Figs. 6 and 9. (The case with the reduced local diffusion coefficient is not included.) Fig. 10 also shows two data points corresponding to the geometric means of data at both the rock matrix sample scale and a tens of meters scale. A test scale of 5 cm is assumed for a rock matrix sample. Note that by definition, Fd is always equal to one at the rock matrix sample scale, and that data point actually represents many overlapped data points because each field-scale data point corresponds to one data point at the rock sample scale. (The data set reported in Zhou et al. (2005) indicates that the geometric means for Fd values are about 10 and 100, respectively, for test scales of tens of meters and hundreds of meters.) We need to keep in

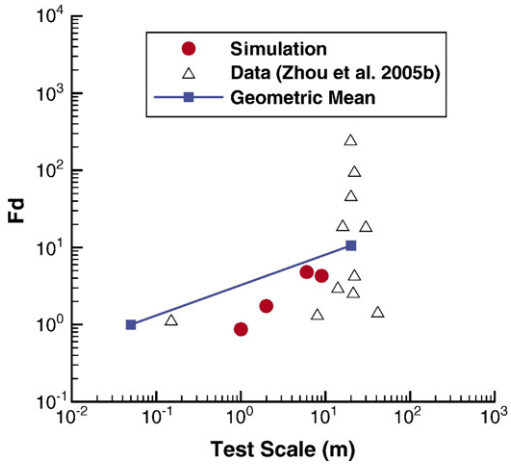

Fig. 10. A comparison between the simulation results with a portion of data from Zhou et al. (2005).

mind that the comparison here is largely qualitative. This is because details of small-scale fractures for the test sites are not available and the assumed high level (small-scale) fractures in our simulations are not necessarily representative for a particular test site. Nevertheless, our simulation results are within the range of the test data. While there is a large degree of fluctuation in Fd data points, the geometric mean of these values for test scales between several meters to 100 m is about 10, as mentioned above. Our simulation result (Fd value) at a scale of about 10 m is 4.3, which is not too far from the geometric mean. Also note that our simulation results are generally on the lower side of the test data (Fig. 10). This may imply that in addition to the effects of flow geometry, other mechanisms also contribute to the scale dependence. As a matter of fact, most recently Liu et al. (2006) theoretically investigated effects of rock matrix heterogeneity on the scale dependence of the effective matrix diffusion coefficient, and found that the heterogeneity indeed potentially contributes to the scale dependence. It is very likely that the scale dependence of the effective matrix diffusion coefficient is a result of a combination of different mechanisms and the flow geometry is one of them. More studies are needed to fully understand this important scale-dependent behavior.

4. Concluding remarks

It has been recognized that matrix diffusion is an important process for retarding solute transport in fractured rock, and the matrix diffusion coefficient is a key parameter for describing this process. Previous studies indicated that the effective matrix diffusion coefficient values, obtained from a number of field tracer tests, are enhanced in comparison with the local values and may increase with test scale. In this study, we have performed numerical experiments to investigate the potential mechanisms behind this scale dependence. The current results indicate that a combination of the local flow loops and the associated matrix diffusion process, together with scaling properties in flow path geometry, seems to be the major mechanism (at a range of scales) for the observed scale dependence of the effective matrix diffusion coefficient. Other potentially important mechanisms may still exist and need to be investigated in future studies.

Acknowledgment

We are indebted to Guoxiang Zhang and Daniel Hawkes at Lawrence Berkeley National Laboratory (LBNL) for their careful review of a preliminary version of this manuscript. We also appreciate the constructive comments from two anonymous reviewers and Dr. E. O. Frind. This report was prepared by LBNL pursuant to a contract funded by the United States Department of Energy (DOE), Office of Civilian Radioactive Waste Management (OCRWM), Office of Science and Technology and International (OST&I) and neither, LBNL nor any of its contractors or subcontractors nor the DOE/OCRWM/OST&I, nor any person acting on behalf of either: makes any warranty or representation, express or implied, with respect to the accuracy, completeness, or usefulness of the information contained in this report, or that the use of any information, apparatus, method, or process disclosed in this report may not infringe privately-owned rights; or assumes any liabilities with respect to the use of, or for damages resulting from the use of, any information, apparatus, method, or process disclosed in this report. Reference herein to any specific commercial product, process, or service by trade name, trademark, manufacturer, or otherwise, does not necessarily constitute or imply its endorsement, recommendation, or favoring by DOE/OCRWM/OST&I. The views, opinions, findings, and conclusions or recommendations of authors expressed herein do not necessarily state or reflect those of the DOE/OCRWM/OST&I.

References

Becker, M.W., Shapiro, A.M., 2000. Tracer transport in fractured crystalline rock: evidence of non-diffusive breakthrough tailing. Water Resour. Res. 36 (7), 1677–1686.

Birgersson, L., Neretnieks, I., 1990. Diffusion in the matrix of granitic rock: field test in the Stripa mine. Water Resour. Res. 26 (11), 2833–2842.

Boving, T.B., Grathwohl, P., 2001. Tracer diffusion coefficients in sedimentary rocks: correlation to porosity and hydraulic conductivity. J. Contam. Hydrol. 53, 85–100.

BSC, 2004. Analyses of Hydrologic Properties Data. ANL-NBS-HS-000042 (Rev 00).

Cvetkovic, V., Painter, S., Outters, N., Selroos, J.-O., 2003. Stochastic simulation of radionuclide migration in discretely fractured rock near Äspö Hard Rock Laboratory. Water Resour. Res. 40, W02404. doi:10.1029/2003WR002655.

Darcel, C., Bour, O., Davy, P., de Dreuzy, J.R., 2003. Connectivity properties of two-dimensional fracture networks with stochastic fractal correction. Water Resour. Res. 39 (10), 1272. doi:10.1029/2002WR001628.

de Dreuzy, J.R., Davy, P., Bour, O., 2001. Hydraulic properties of two-dimensional random fracture networks following a power law length distribution: 1. Effective connectivity. Water Resour. Res. 37 (8), 2065–2078.

de Marsily, G., 1986. Quantitative Hydrogeology. Academic, San Diego, Calif.

Finsterle, S., 1999. ITOUGH2 User's Guide. Report LBNL-40040, UC-400. Lawrence Berkeley National Laboratory, Berkeley, CA.

Frind, E.O., Sudicky, E.A., Schellenberg, S.L., 1987. Micro-scale modeling in the study of plume evolution in heterogeneous media. Stoch. Hydrol. Hydraul. 1 (4), 263–279.

Gelhar, L.W., 1993. Stochastic Subsurface Hydrology. Prentice Hall, New York.

Jardine, P.M., Sanford, W.E., Gwo, J.P., Reedy, O.C., Hicks, D.S., Riggs, J.S., Bailey, W.B., 1999. Quantifying diffusive mass transfer in fractured shale bedrock. Water Resour. Res. 35 (7), 2015–2030.

Karasaki, K., Freifeld, B., Cohen, A., Grossenbacher, K., Cook, P., Vasco, D., 2000. A multidisciplinary fractured rock characterization study at Raymond field site, Raymond. CA. J. Hydrol. 236 (1–2), 17–34.

Liu, H.H., Bodvarsson, G.S., Finsterle, S., 2002. A note on unsaturated flow in two-dimensional fracture network. Water Resour. Res. 38 (9), 1176. doi:10.1029/2001WR000977.

Liu, H.H., Haukwa, C.B., Ahlers, C.F., Bodvarsson, G.S., Flint, A.L., Guertal, W.B., 2003. Modeling flow and transport in unsaturated fractured rock: an evaluation of the continuum approach. J. Contam. Hydrol. 62–63, 173–188.

Liu, H.H., Salve, R., Wang, J.S., Bodvarsson, G.S., Hudson, D., 2004a. Field investigation into unsaturated flow and transport in a fault: model analyses. J. Contam. Hydrol. 74 (1–4), 39–59.

Liu, H.H., Bodvarsson, G.S., Zhang, G., 2004b. Scale dependency of the effective matrix diffusion coefficient. Vadose Zone J. 3, 312–315.

Liu, H.H., Zhang, Y.Q., Molz F.J., 2006. Scale dependency of the effective matrix diffusion coefficient: Some analytical results. Vadose Zone J. (in review).

Maloszewski, P., Herrmann, A., Zuber, A., 1999. Interpretation of tracer tests performed in a fractured rock of the Lange Bramke Basin, Germany. Hydrogeol. J. 7, 209–218.

Mazurek, M., Bossart, P., Hermanson, J., 2001. Classification and characterization of water conducting features at Äspö. Proceedings of International Semina First TRUE stage, Rep. TR-01-24. Swed. Nucl. Fuel and Waste Manag. Co. (SKB), Stocholm, pp. 203–208.

Neretnieks, I., 2002. A stochastic multi-channel model for solute transport-analysis of tracer tests in fractured rock. J. Contam. Hydrol. 55, 175–211.

Neretnieks, I., Moreno, L., 2003. Prediction of some in situ tracer tests with sorbing tracers using independent data. J. Contam. Hydrol. 61, 351–360.

Neuman, S.P., 1990. Universal scaling of hydraulic conductivities and dispersivities in geologic media. Water Resour. Res. 26 (8), 1749–1758.

Painter, S., Cvetkovic, V., 2005. Upscaling discrete fracture network simulations: an alternative to continuum transport models. Water Resour. Res. 41, W02002. doi:10.1029/2004WR003682.

Polak, A., Grader, A.S., Wallach, R., Nativ, R., 2003. Chemical diffusion between a fracture and the surrounding matrix: measurement by computed tomography and modeling. Water Resour. Res. 39 (4), 1106. doi:10.1029/2001WR000813.

Reimus, P.W., Haga, M.J., Adams, A.I., Callahan, T.J., Turin, H.J., Counce, D.A., 2003a. Testing and parameterizing a conceptual solute transport model in saturated fractured tuff using sorbing and nonsorbing tracers in cross-hole tracer tests. J. Contam. Hydrol. 62–63, 613–636.

Reimus, P., Pohll, G., Mihevc, T., Chapman, J., Haga, M., Lyles, B., Kosinski, S., Niswonger, R., Sanders, P., 2003b. Testing and parameterizing a conceptual model for solute transport in a fractured granite using multiple tracers in a forced-gradient test. Water Resour. Res. 39 (12), 1356. doi:10.1029/2002WR001597.

Renshaw, C.E., 1999. Connectivity of joint networks with power law length distributions. Water Resour. Res. 35 (9), 2661–2670.

Sánchez-Vila, X., Carrera, J., 2004. On the striking similarity between the moments of breakthrough curves for heterogeneous medium and a homogeneous medium with a matrix diffusion term. J. Hydrol. 294, 164–175.

Shapiro, A.M., 2001. Effective matrix diffusion in kilometer-scale transport in fractured crystalline rock. Water Resour. Res. 37 (3), 507–522.

Staffer, D., Aharony, A., 1994. Introduction to Percolation Theory. Taylor & Francis, Bristol, PA.

Tang, D.H., Frind, E.O., Sudicky, E.A., 1981. Contaminant transport in a fractured porous media: analytical solution for a single fracture. Water Resour. Res. 17 (3), 555–564.

Tsang, C.F., Doughty, C., 2003. A particle-tracking approach to simulating transport in a complex fracture. Water Resour. Res. 39 (7), 1174. doi:10.1029/2002WR001614.

Tsang, C.F., Neretnieks, I., 1998. Flow channeling in heterogeneous fractured rocks. Rev. Geophys. 36 (2), 275–298.

Wu, Y.S., Liu, H.H., Bodvarsson, G.S., 2004. A triple-continuum approach for modeling flow and transport processes in fractured rock. J. Contam. Hydrol. 73, 145–179.

Zhou, Q., 2005. Software Management Report for iTOUGH2-TRAT. Lawrence Berkeley National Laboratory, Berkeley.

Zhou Q., Liu, H.H., Molz, F.J., Zhang, Y., Bodvarsson, G.S., 2005. Effective matrix diffusion coefficient for fractured rock: Results from a literature survey (in review).

Zhou, Q., Liu, H.H., Molz, F.J., Bodvarsson, G.S., 2006. Evidence of multi-process matrix diffusion in a single fracture from a field tracer test. Transp. Porous Media 63, 473–487.